

# PCCP

Accepted Manuscript



This is an *Accepted Manuscript*, which has been through the Royal Society of Chemistry peer review process and has been accepted for publication.

*Accepted Manuscripts* are published online shortly after acceptance, before technical editing, formatting and proof reading. Using this free service, authors can make their results available to the community, in citable form, before we publish the edited article. We will replace this *Accepted Manuscript* with the edited and formatted *Advance Article* as soon as it is available.

You can find more information about *Accepted Manuscripts* in the [Information for Authors](#).

Please note that technical editing may introduce minor changes to the text and/or graphics, which may alter content. The journal's standard [Terms & Conditions](#) and the [Ethical guidelines](#) still apply. In no event shall the Royal Society of Chemistry be held responsible for any errors or omissions in this *Accepted Manuscript* or any consequences arising from the use of any information it contains.

Cite this: DOI: 10.1039/c0xx00000x

www.rsc.org/xxxxxx

ARTICLE TYPE

## $\beta$ -Isocyanoalanine as an IR probe: comparison of vibrational dynamics between isonitrile and nitrile-derivatized IR probes

Michał Maj,<sup>‡ab</sup> Changwoo Ahn,<sup>‡b</sup> Dorota Kossowska,<sup>ab</sup> Kwanghee Park,<sup>ab</sup> Kyungwon Kwak,<sup>c</sup>  
Hogyu Han<sup>\*b</sup> and Minhaeng Cho<sup>\*ab</sup>

Received (in XXX, XXX) Xth XXXXXXXXX 20XX, Accepted Xth XXXXXXXXX 20XX

DOI: 10.1039/b000000x

An infrared (IR) probe based on isonitrile (NC)-derivatized alanine **1** was synthesized and the vibrational properties of its NC stretch mode were investigated by FTIR and femtosecond IR pump–probe spectroscopy. It is found that the NC stretch mode is very sensitive to the hydrogen-bonding ability of solvent molecules. Moreover, its transition dipole strength is larger than that of nitrile (CN) in nitrile-derivatized IR probe **2**. The vibrational lifetime of the NC stretch mode is found to be  $5.5 \pm 0.2$  ps in both D<sub>2</sub>O and DMF solvents, which is several times longer than that of the azido (N<sub>3</sub>) stretch mode in azido-derivatized IR probe **3**. These properties altogether suggest that the NC group can be a very promising sensing moiety of IR probes for studying solvation structure and dynamics of biomolecules.

### Introduction

Owing to the development of infrared (IR) spectroscopy in the ultrafast regime, it becomes possible to measure local electric field and its gradients around an IR probe. To extract site-specific information on protein structure, function and dynamics, IR probes based on amino acids, which act like an antennae sensing local electrostatic environment, have been introduced site-specifically into proteins.<sup>1–10</sup>

A variety of modified amino acids containing vibrationally active moieties such as nitrile,<sup>11–14</sup> azido,<sup>15–17</sup> thiocyanato<sup>18–20</sup> and selenocyanato groups have been reported. Although many IR probes have been found to be of use in FTIR studies, their use in time-resolved nonlinear IR investigations is markedly limited by a few drawbacks in spectral properties. A desirable IR probe should possess certain characteristics like high sensitivity to the local environment change, narrow bandwidth for less spectral congestion, large transition dipole strength for good signal to noise ratio and properly long vibrational lifetime. Moreover, the vibrationally active group incorporated into amino acids should not significantly perturb the native structure and dynamics of the protein of interest.

Getahun et al. showed that cyanoalanine and cyanophenylalanine, where the latter has been widely used as a fluorescent probe too,<sup>21–23</sup> are useful IR probes.<sup>24</sup> Although the nitrile group was found to be a highly sensitive reporter of local solvation, its application to studying ultrafast dynamics of proteins is highly limited due to very small transition dipole strength,<sup>1,25,26</sup> especially when the nitrile group is attached to an aliphatic side chain as in cyanoalanine.

Recently, the CN stretch mode of the thiocyanato group has been paid much attention since this group can be introduced site-specifically into proteins by direct conversion of their cysteine thiol group.<sup>27–31</sup> Park et al. showed that the CN stretch modes in thiocyanato- and selenocyanato-derivatized prolines have significantly longer vibrational lifetimes than any other vibrational modes in various IR probes reported so far.<sup>32</sup> However, still due to their weak transition dipole strengths, nonlinear IR spectroscopic signals are very weak, limiting their application to studying nonequilibrium protein dynamics in condensed phases.

In parallel, some interesting studies with azido-derivatized amino acids,<sup>25,33,34</sup> nucleotides<sup>35,36</sup> and proteins<sup>4,5,37–40</sup> have been reported. The asymmetric stretch mode of the azido group has

notably large transition dipole strength as compared to those of the nitrile, thiocyanato and selenocyanato groups. Furthermore, its frequency is found to be very sensitive to local electric field produced by polar groups in solutions and proteins. Consequently, various azido-derivatized biomolecules have been under investigation using time-resolved IR pump-probe and 2DIR methods.<sup>6,37,41-44</sup> Nevertheless, the azido group still has certain drawbacks. First, its size is a bit larger than that of nitrile. Second, due to its polar character, the azido group can introduce a large perturbation to the backbone structures of polypeptides and proteins, which essentially affects their native structural propensities.<sup>45</sup> Lee et al. showed that azido-derivatized prolines can have multiple conformations that are mainly modulated by the intramolecular interactions between the azido group and backbone peptides.<sup>34,46</sup> Third, the fundamental transition band of the asymmetric azido stretch mode is often overlapped with other accidental Fermi resonance bands,<sup>26,34,36,47-49</sup> which makes quantitative spectral band analysis difficult.

Another interesting probes that can be applied to studying structure and dynamics of proteins are metal carbonyls. One of the popular carbonyl compounds that has been applied in many studies is tungsten hexacarbonyl, W(CO)<sub>6</sub>.<sup>50-53</sup> Its large IR intensity has been found to be one of the advantages over the other commonly used probes. However, due to extremely low solubility in water, its application has been limited to studying relatively nonpolar environments. Recently, Peran et al. and Woys et al. have proposed new ways of introducing metal tricarbonyl into proteins through site-specific mutagenesis, allowing the carbonyl compounds to be used in aqueous environments.<sup>54,55</sup> Besides significantly large intensity, the carbonyl probes have vibrational lifetimes that are sensitive to local environment. One of possible drawbacks of the carbonyl probes is their sizes, which could introduce some perturbations to structure and dynamics of studied proteins when they are introduced into hydrophobic parts of proteins.

Here, we report a novel IR probe based on isonitrile (NC)-derivatized alanine **1** (Ac-Ala(NC)-NHMe, Fig. 1). The vibrational properties of **1** were investigated by FTIR and femtosecond IR pump-probe spectroscopy. The experimental results were directly compared with those of nitrile (CN)-derivatized alanine **2** (Ac-Ala(CN)-NHMe, Fig. 1) and azido (N<sub>3</sub>)-derivatized alanine **3** (Ac-Ala(N<sub>3</sub>)-NHMe, Fig. 1).

Applicability of the isonitrile probe to study the vibrational dynamics of biomolecules is further discussed.

## Experimental section

### Materials

Compounds **0-3** were synthesized and characterized (Scheme 1 and Section S1 of the ESI†). Various solvents including D<sub>2</sub>O and DMF were purchased from Sigma-Aldrich and used as received. For FTIR and IR pump-probe experiments, all samples were placed in a home-made IR cell with two 3 mm thick CaF<sub>2</sub> windows and a 25 μm thick Teflon spacer. The concentration of the sample solution used in femtosecond IR pump-probe measurements was set at 0.3 M.

### FTIR spectroscopy

FTIR spectra were measured on a Bruker VERTEX 70 spectrometer. FTIR spectra were measured with a frequency resolution of 1 cm<sup>-1</sup> at 22 °C.

### Polarization-controlled IR pump-probe spectroscopy

Experimental details on polarization-controlled IR pump-probe spectroscopy and the femtosecond laser setup used for the present measurements have been described elsewhere.<sup>56</sup> In brief, a train

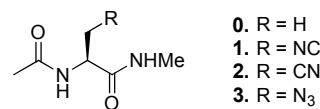
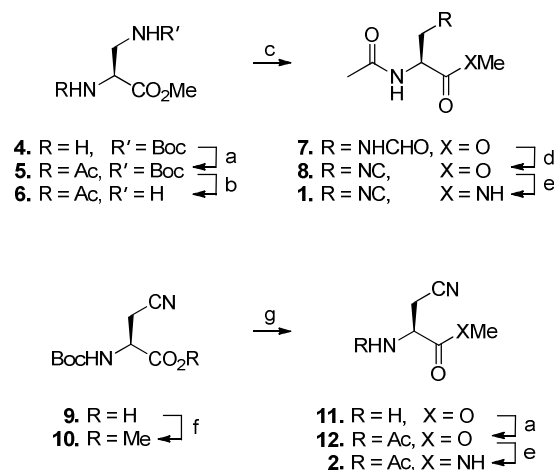


Fig. 1 Structures of compounds **0-3** used for IR study.



Scheme 1 Syntheses of **1** and **2**.<sup>a</sup>

<sup>a</sup>Reagents and conditions: (a) Ac<sub>2</sub>O, Et<sub>3</sub>N, CH<sub>2</sub>Cl<sub>2</sub>, rt, (**5**, 97%; **12**, 47%); (b) TFA, rt, 94%; (c) TFEF, HCO<sub>2</sub>Na, THF, rt, 79%; (d) POCl<sub>3</sub>, Et<sub>3</sub>N, CH<sub>2</sub>Cl<sub>2</sub>, -30 °C, 51%; (e) 40% MeNH<sub>2</sub>, MeOH, rt, (**1**, 71%; **2**, 87%); (f) MeI, K<sub>2</sub>CO<sub>3</sub>, DMF, rt, 84%; (g) 4 N HCl, 1,4-dioxane, rt, 92%.

of 800 nm pulses generated by femtosecond Ti:sapphire oscillator (Tsunami, Spectra-Physics) and regenerative amplifier (Spitfire, Spectra-Physics) are used to pump an optical parametric amplifier (OPA) to produce near IR pulses centered at  $\sim 1.4 \mu\text{m}$  and  $\sim 1.9 \mu\text{m}$ . Then the generated near IR pulses are focused onto 2.0 mm thick AgGaS<sub>2</sub> crystal to produce mid-IR pulses through difference frequency generation process. The mid-IR pulses are afterwards split by ZnSe beam splitter into pump and time-delayed probe pulses with intensity ratio of 9:1 and focused onto a sample. The time delay between those two pulses is controlled by a motorized linear stage placed in the probe beam line. The pump-probe signal is frequency-resolved with monochromator and detected at each time delay by 64-element MCT array detector. The average power of the pump pulse, measured in front of the sample, was  $\sim 450 \mu\text{W}$ .

The intensity of the signal decays as the time delay increases due to both vibrational and orientational relaxation processes. To separate the vibrational and orientational contributions to the decaying signal, we had to measure the pump-probe signals with two different polarizations of the probe beams with respect to the polarization direction of the pump beam, i.e., parallel  $S_{\parallel}(t)$  and perpendicular  $S_{\perp}(t)$  signals. From them, we can obtain both isotropic and anisotropic signals responsible for vibrational population and orientational relaxations, respectively:

$$S_{\text{iso}}(t) = S_{\parallel}(t) + 2S_{\perp}(t) = 3P(t) \quad (1)$$

$$S_{\text{aniso}}(t) = S_{\parallel}(t) - S_{\perp}(t) = r(t)P(t) \quad (2)$$

## Results and discussion

### FTIR spectroscopy

To show how sensitive the isonitrile group is to the polarity and hydrogen-bonding ability of solvent, the FTIR spectra of **1** in the NC stretch region were investigated with a variety of solvents (Fig. 2). They range from highly strong H-bond-donating (CF<sub>3</sub>CH<sub>2</sub>OH), strongly H-bonding (D<sub>2</sub>O and MeOH) and weakly interacting (CHCl<sub>3</sub>) to even H-bond-accepting (MeOAc, THF and DMF) solvents. The detailed analysis results of the FTIR spectra are given in the ESI, Table S1. It is apparent that the isonitrile group is a highly sensitive reporter of H bonding.

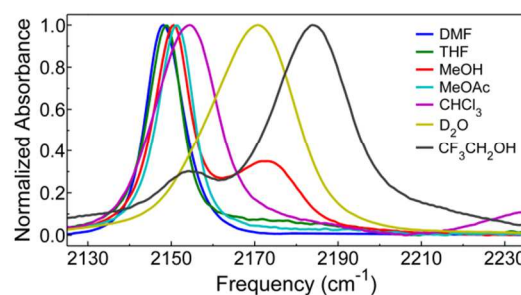


**Fig. 2** Isonitrile (NC) stretch FTIR spectra of **1** in various solvents. For the fitting parameters, see Table S1 of the ESI.†

The FTIR spectra of **1** in the non-H-bonding solvents are very similar to those reported by Levinson et al. for isotopically labelled benzonitrile.<sup>57</sup> The isonitrile peak frequencies of **1** in three non-H-bonding solvents (MeOAc, THF and DMF) are in the range from 2148 to 2151 cm<sup>-1</sup> and the spectral bandwidth (FWHM) is  $\sim 10 \text{ cm}^{-1}$ . Although the polarities of these three aprotic solvents are significantly different from one other – note that the dielectric constants of DMF and MeOAc are 36.7 and 6.7, respectively – the NC stretch IR spectra are found to be quite similar.

Now, among the H-bonding solvents, CHCl<sub>3</sub> has been known to make a weak C–H H-bonding interaction with H-bond acceptor. The formation of such weak H bond results in small but apparent blue-shift of NC frequency to 2154 cm<sup>-1</sup> as well as significant broadening of the bandwidth ( $\sim 17 \text{ cm}^{-1}$ ), in comparison to those in non-H-bonding solvents. Following the increase of H-bonding strength, the NC frequency is further blue-shifted and its magnitude is approximately proportional to the H-bond-donating ability of solvents.<sup>58</sup> In D<sub>2</sub>O, a large frequency blue-shift of  $\sim 20 \text{ cm}^{-1}$  and a substantial broadening of the bandwidth ( $\sim 24 \text{ cm}^{-1}$ ) are observed. The NC stretch IR spectra of **1** in MeOH and CF<sub>3</sub>CH<sub>2</sub>OH appear to be complicated. First of all, the spectrum in MeOH shows a doublet with a relatively weak blue-shifted peak – note that the CN stretch IR spectrum of acetonitrile in MeOH also exhibits a doublet feature but with more or less equal intensities.<sup>59</sup> Nonetheless, these two peaks can still be attributed to the free (2150 cm<sup>-1</sup>) and singly H-bonded (2173 cm<sup>-1</sup>) NC, because the high frequency peak position is close to that in D<sub>2</sub>O.

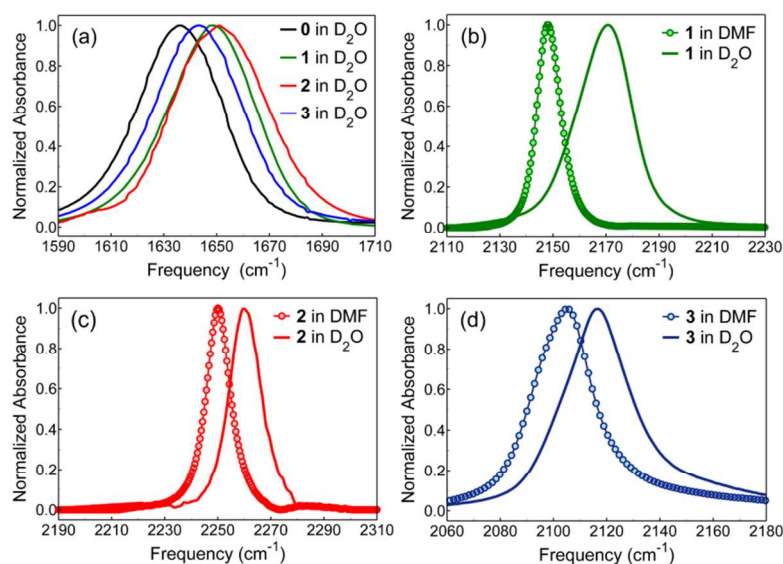


**Fig. 3** (a) Amide I' FTIR spectra of **0–3** in D<sub>2</sub>O. (b–d) Isonitrile (NC), nitrile (CN), and azido (N<sub>3</sub>) stretch FTIR spectra of **1–3** in DMF and D<sub>2</sub>O. Background subtracted spectra are presented in (b)–(d). For the fitting parameters, see Table S1 of the ESI† (a) and Table 1 (b–d). Factor analyses for (d) are shown in Fig. S2 of the ESI†

What is particularly noteworthy is that the peak separation between two NC bands of **1**, which is 23 cm<sup>-1</sup>, is much larger than that between two CN bands of acetonitrile. This observation may indicate that either H-bonding interaction of MeOH with  
 5 isonitrile is stronger or isonitrile frequency or its stretch potential energy curve is more sensitive to the presence of H-bonding interaction. Interestingly, when CF<sub>3</sub>CH<sub>2</sub>OH is used, the high  
 10 frequency peak of the doublet becomes dominant and shows further blue-shift to 2184 cm<sup>-1</sup>. This indicates that the OH group of CF<sub>3</sub>CH<sub>2</sub>OH is the strongest H-bond donor among the solvent  
 15 considered here, which is consistent with the Kamlet-Taft parameter<sup>58</sup> (Fig S1 of the ESI†) as well as the previous results on the thiocyanato group.<sup>28,60–62</sup> This shows that the isonitrile probe is especially sensitive to the H bond of the OH group in water and

Similar to the trend of NC frequency shift with respect to solvent H-bond strength, the experimentally measured lineshapes are also related to it. The bandwidths of NC stretch IR spectra in non-H-bonding solvents are quantitatively similar to one another,  
 20 but it generally increases from ~17 to ~22 cm<sup>-1</sup> as the solvent H-bonding ability increases.<sup>58</sup> Unlike the NC stretch IR spectra of **1** in MeOH and CF<sub>3</sub>CH<sub>2</sub>OH, which are characterized by two distinct peaks, that in D<sub>2</sub>O is broad and featureless due to the spectral overlap of peaks originating from various H-bonding  
 25 configurations.

For the sake of the ultrafast IR pump–probe measurements and comparison with other derivatized alanine systems, D<sub>2</sub>O and DMF solvents were specifically chosen for our study since these two solvents could represent H-bonding and non-H-bonding  
 30 environments in proteins, respectively. Note that DMF has relatively high dielectric constant so that it is a strongly polar solvent without H-bond-donating ability. The FTIR spectra of **0–3** in both D<sub>2</sub>O and DMF were measured and the normalized background subtracted spectra are presented in Fig. 3. The NC  
 35 (CN) and azido stretch IR spectra were investigated together with the amide I' IR spectra.

The amide I' bands of **1** and **2** show a single peak that is well characterized by a single Voigt profile and its frequency is 15 cm<sup>-1</sup> blue-shifted from that of alanine **0** (Ac-Ala-NHMe) (Fig. 3a  
 40 and Table S1 of the ESI†). This indicates that the introduction of either isonitrile or nitrile group may result in some perturbation to the backbone conformation of **0** or change in its local solvation. However, the fact that only a single symmetric peak was observed in each case indicates that the backbone conformation  
 45 or solvation has no notable heterogeneity. Contrary to the finding in the IR spectrum of (4*S*)-azidoproline, where the amide I' band is split into several distinct components, β-azidoalanine **3** shows a single symmetric peak at slightly blue-shift (~7 cm<sup>-1</sup>) position in comparison to that of **0** and its bandwidth is similar to that of **1**.<sup>34</sup>

**Table 1** Spectral properties of 1–3<sup>a</sup>

	1		2		3	
	D <sub>2</sub> O	DMF	D <sub>2</sub> O	DMF	D <sub>2</sub> O	DMF
$\omega_{\text{center}}$ (cm <sup>-1</sup> )	2169.5	2151.6	2260.4	2250.2	2116.1	2103.6
FWHM (cm <sup>-1</sup> )	24.1	10.6	14.3	11.0	29.0	26.4
$\epsilon$ (cm <sup>-1</sup> M <sup>-1</sup> )	142	390	14	27	349	333
D <sup>b</sup> (10 <sup>-2</sup> Debye <sup>2</sup> )	1.82	2.21	0.06	0.15	5.49	4.80
$T_1$ (ps)	5.52±0.18	5.53±0.17	-	-	1.14±0.04 (0.10) <sup>d</sup>	1.34±0.08 (0.10) <sup>d</sup>
$\tau_{\text{or}}$ (ps)	10.33±2.24 <sup>c</sup> 0.52±0.20	7.28±0.94	-	-	0.13±0.01 (0.24) <sup>d</sup>	0.065±0.004 (0.15) <sup>d</sup>

<sup>a</sup>Fitting parameters obtained from Figs. 3b–d ( $\omega_{\text{center}}$ , FWHM,  $\epsilon$  and D), 5b and 6b ( $T_1$ ) and 5c and 6c ( $\tau_{\text{or}}$ ). <sup>b</sup>ref. 72. <sup>c</sup>major component. <sup>d</sup>amplitudes.

Although the NC and CN stretch bands of **1** and **2** exhibit a single symmetric peak (Fig. 3b and c), their vibrational properties are quantitatively different (Table 1). First of all, the center frequency of the NC stretch is red-shifted by  $\sim 100$  cm<sup>-1</sup> in comparison to that of the CN stretch in both solvents. Such red-shift is definitely advantageous because the NC peak is farther away from the broad OD stretch band in D<sub>2</sub>O solution, which makes nonlinear IR spectroscopic studies of NC probe easier without undesired background absorption by D<sub>2</sub>O. Often, to eliminate such high background level at peak maximum of the CN stretch band, either single or double isotopic labelling of the nitrile group was needed, which is expensive.<sup>57,62</sup> Moreover, the synthetic route used in the present work allows for isotopic labelling of the isonitrile group as well, consequently shifting the band further to the region where the absorbance of the OD stretch is negligibly small. In H<sub>2</sub>O, the IR pump–probe signals in the frequency ranges of these IR probes are often heavily contaminated with strong heat contributions from vibrational excitations of broad combination (H<sub>2</sub>O bending + water intermolecular vibrations) modes at around 2100 cm<sup>-1</sup>.<sup>63,64</sup>

The N<sub>3</sub> stretch band of **3** exhibits also a single peak but, in contrast to the NC and CN stretch bands, the spectrum is asymmetric in lineshape (Fig. 3d). It is likely that the source of asymmetric lineshape is the overlap of the N<sub>3</sub> stretch band with a peak originating from accidental Fermi resonance with one of the overtone or combination bands (for factor analyses, see Fig S2 of the ESI†). The centre frequency of the N<sub>3</sub> stretch is red-shifted by  $\sim 50$  cm<sup>-1</sup> and  $\sim 150$  cm<sup>-1</sup> in comparison to that of the NC and CN stretch, respectively (see Table 1). Such substantial red-shift of the N<sub>3</sub> stretch with respect to nitriles is, together with its large intensity, one of the advantages of the azido probes.

What appears to be the most interesting feature of our new probe **1** is its large dipole strength that allows for measuring the spectra at relatively low concentrations. The dipole strength of the NC stretch mode is  $1.82\text{--}2.21 \times 10^{-2} \text{ D}^2$ , which is 5–40 times larger than that of the CN stretch modes in various CN-derivatized IR probes and is only about 2–3 times smaller than that of the azido stretch mode. It is noteworthy that a number of different azido-derivatized IR probes have been used and their transition intensities were found to be larger than that of **3** depending on the type of molecule to which the azido group is attached.<sup>17,65</sup> Although the dependence of transition intensity of isonitrile on attached molecular structure has not been investigated yet, it is possible that the intensity differences between azido and isonitrile probes are larger than the one reported here. The origin of large increase in transition dipole strength can be attributed to the hyperconjugation between the  $\sigma$  bonding orbital of the C–H bond and the  $\pi^*$  antibonding orbital of the neighbouring NC group. The electronic structure of NC indicates that the nitrogen atom possesses partially positive charge and the terminal carbon has partially negative charge. This makes the electronic structure of NC unstable compared to that of CN. Thus, the lower-lying  $\pi^*$  antibonding orbital of NC is placed energetically close to the  $\sigma$  bonding orbital of C–H, which enhances the hyperconjugation and increases the antibonding character of NC compared to CN. This model also supports that the observed red-shift comes from the weakening of triple bond character due to the increase of antibonding character with hyperconjugation. Thus, we believe that isonitrile may serve as a great probe for studying ultrafast dynamics of biomolecules with time-resolved IR pump–probe measurement method.

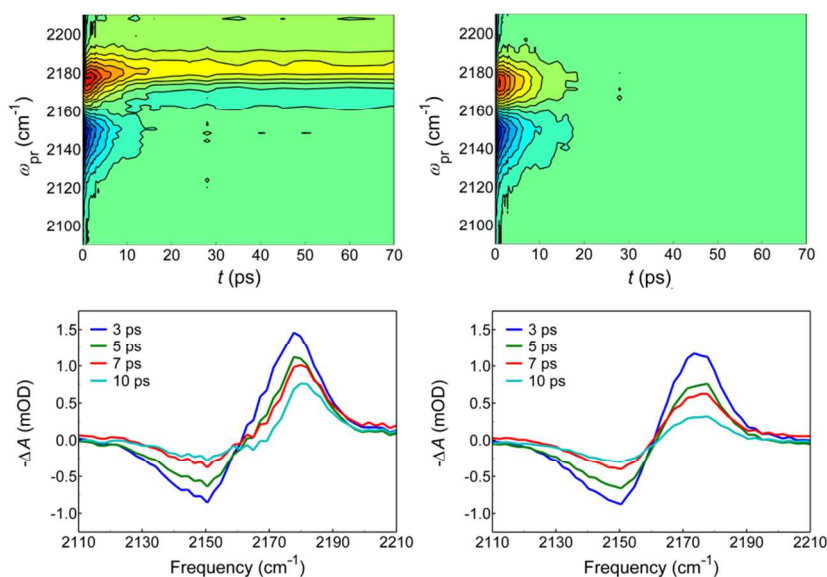


**Fig. 4** Time- and frequency-resolved isotropic IR pump-probe signals (upper) and their slice spectra (lower) at the delay time  $t$  for **1** in D<sub>2</sub>O before (left) and after (right) subtraction of the heat contribution.

#### Polarization-controlled IR pump-probe spectroscopy

To determine the vibrational and orientational relaxation lifetimes of the NC stretch mode, we carried out polarization-controlled IR pump-probe (IR PP) measurements for **1**. For direct comparisons, the same measurements were carried out for the N<sub>3</sub> stretch mode of **3**. Due to the very low transition dipole strength of the CN stretch mode, it was impossible to obtain good quality signal for **2**. Frequency-resolved IR PP signals for **1** in D<sub>2</sub>O are presented in Fig. 4. The IR PP signal consists of both positive and negative contributions that originate from different transition pathways. The positive peak results from the ground-state bleach ( $\nu = 0 \rightarrow 1$  transition) and stimulated emission ( $\nu = 1 \rightarrow 0$  transition), whereas the negative peak results from the excited-state absorption ( $\nu = 1 \rightarrow 2$  transition).

Although the energy relaxation process should make the signal eventually decay to zero, finite residual signal originating from pump-induced heating effect was observed (Fig. S3 of the ESI†).<sup>66</sup> Heating signal usually makes it difficult to accurately determine vibrational lifetimes. Here, we eliminate the heating contribution to the isotropic IR PP signal by assuming that it is a rising function:

$$h(t) = \left( 1 - \exp\left(-\frac{t}{T_{\text{heat}}}\right) \right) \quad (3)$$

Since the IR PP signal at long delay times is dictated by the heating component, the corrected IR PP signal is obtained by subtracting the scaled signal at long times from the raw signal as

$$P(\omega, t) = S_{\text{iso}}(\omega, t) - h(t) S_{\text{iso}}(\omega, \infty) \quad (4)$$

The only remaining parameter that needs to be chosen is exponential time constant  $T_{\text{heat}}$  representing the local heating process. If we assume that the local heating occurs mainly due to the relaxation of the OD stretch mode of D<sub>2</sub>O solvent molecules we can apply the literature value of  $T_{\text{heat}} = \sim 0.9$  ps.<sup>7</sup> The IR PP signals before and after subtraction with this time constant are presented in Fig. 4 upper, which shows that heating contribution was successfully removed. Slice spectra at several delay times shows symmetric shape with approximately equal 0–1 and 1–2 transition peak intensities. Furthermore, this correction scheme with eqn (4) also works well in removing the background signal (compare the left and right slice spectra in Fig. 4 lower).

The heating contribution-free isotropic IR PP signals for **1** and **3** in D<sub>2</sub>O and DMF were obtained (Fig. S4 of ESI†) and their slice spectra at each delay time (Figs. 5a and 6a) were fitted to two Gaussian functions for the 0–1 and 1–2 transition peaks. The vibrational lifetimes were obtained from the time profiles of the integrated peak areas of the positive (0–1) and negative (1–2) peaks. In the case of **1**, the vibrational population decays were well-characterized by a single-exponential function, where the vibrational lifetimes were determined to be  $5.52 \pm 0.18$  ps and  $5.53 \pm 0.17$  ps in D<sub>2</sub>O and DMF, respectively (Fig. 5b). Here, it should be noted that the positive and negative peak areas could be

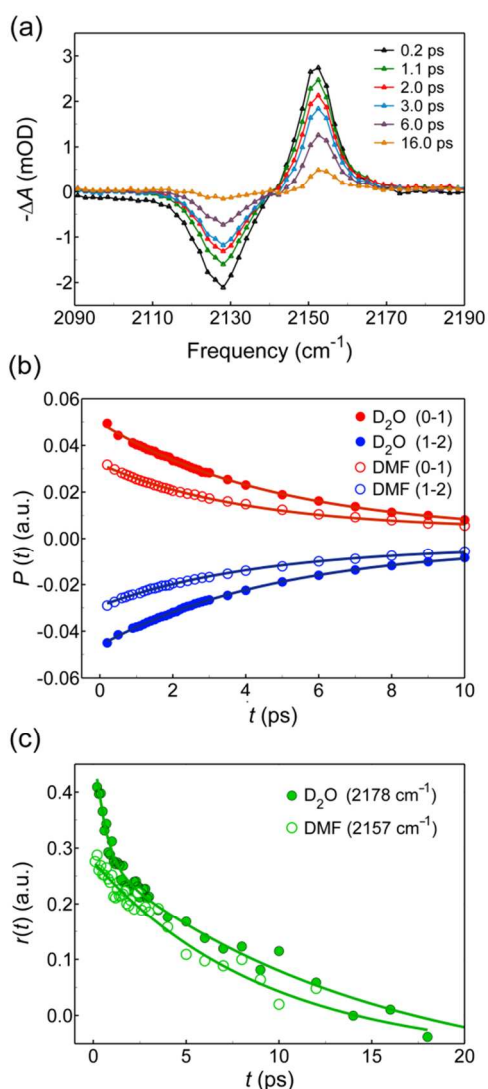


**Fig. 5** Polarization-controlled IR pump-probe data of **1**. (a) Isotropic IR pump-probe spectra of **1** in DMF at the delay time  $t$ . (b) Vibrational population decays of **1** in D<sub>2</sub>O and DMF. The integrated peak areas of the positive (0–1) and negative (1–2) peaks of the isotropic IR pump-probe spectra were fitted to a single-exponential decay function for both D<sub>2</sub>O and DMF solutions. (c) Anisotropy decays of **1** in D<sub>2</sub>O and DMF. The anisotropic signals at the probe frequency were fitted to a biexponential (D<sub>2</sub>O solution) or single-exponential (DMF solution) decay function. For the fitting parameters, see Table 1.

quantitatively measured mainly because the peak-to-peak frequency difference is large due to large anharmonicity of the NC group compared with the bandwidth. In many IR PP experiments, reliable and independent estimations of 0–1 and 1–2 peak areas have often been hampered by destructive interference between them. However, the NC probe provides sufficiently large peak separation so that this new IR probe opens the possibility to separately observe the dynamics of molecules in vibrationally excited and ground states without relying on model based fitting analysis. The observation of nearly identical vibrational lifetimes in both D<sub>2</sub>O and DMF, indicates that intramolecular vibrational

relaxation is the dominant relaxation process for the NC stretch mode.

For **3**, the vibrational population decays were characterized by a biexponential function, where the vibrational lifetimes were determined to be  $1.14 \pm 0.04$  ps and  $0.13 \pm 0.01$  ps in D<sub>2</sub>O and  $1.34 \pm 0.08$  and  $0.065 \pm 0.004$  ps in DMF (Fig. 6b). In addition, the amplitude of the short time component is quite large (see Table 1), which indicates that the majority of the signal decays in sub-picosecond timescale after the excitation. However, it should be noted that the duration of the mid-IR pulse used in our experiments is  $\sim 60$  fs so that there exists an uncertainty in determining time constants that are comparable to or even shorter than the pulse duration time. The vibrational lifetime of the NC stretch mode is found to be several times longer in comparison to that of the azido stretch mode and also longer than that of the CN stretch mode in cyanophenylalanine.<sup>67–69</sup>

The orientational relaxation time constants were estimated from anisotropic signals at certain probe frequencies. For **1** in D<sub>2</sub>O, the orientational relaxation time constant was obtained by taking the average value for the anisotropic signals in the probe frequency range from 2178 to 2184 cm<sup>-1</sup> (Fig. 5c). All the anisotropy decays show a biexponential pattern with time constants of  $0.52 \pm 0.20$  ps and  $10.33 \pm 2.24$  ps and with almost equal amplitudes. In the case of DMF solution, the anisotropic signals in the probe frequency range from 2150 to 2156 cm<sup>-1</sup> were used to determine the orientational relaxation time constant. Contrary to the anisotropy decay in D<sub>2</sub>O, that in DMF is found to be well-described by a single-exponential function with a time constant of  $7.28 \pm 0.94$  ps. In the case of **3**, the anisotropic signals in the probe frequency range of 2115–2125 and 2104–2113 cm<sup>-1</sup> were used for D<sub>2</sub>O and DMF solutions, respectively. It is found that the anisotropy decays are well-described with a single-exponential function with time constants of  $4.50 \pm 0.95$  ps and  $3.82 \pm 1.98$  ps in D<sub>2</sub>O and DMF, respectively (Fig. 6c).

The orientational relaxation time constants can be related to the local solvation structure around the vibrational probe. In DMF, the anisotropic signal at time zero is slightly different from 0.4. Such deviation could originate from inertial orientational relaxation component that decays within the duration of the probe pulse and it cannot be resolved using our experimental setup. Interestingly, the inertial component is significantly smaller in



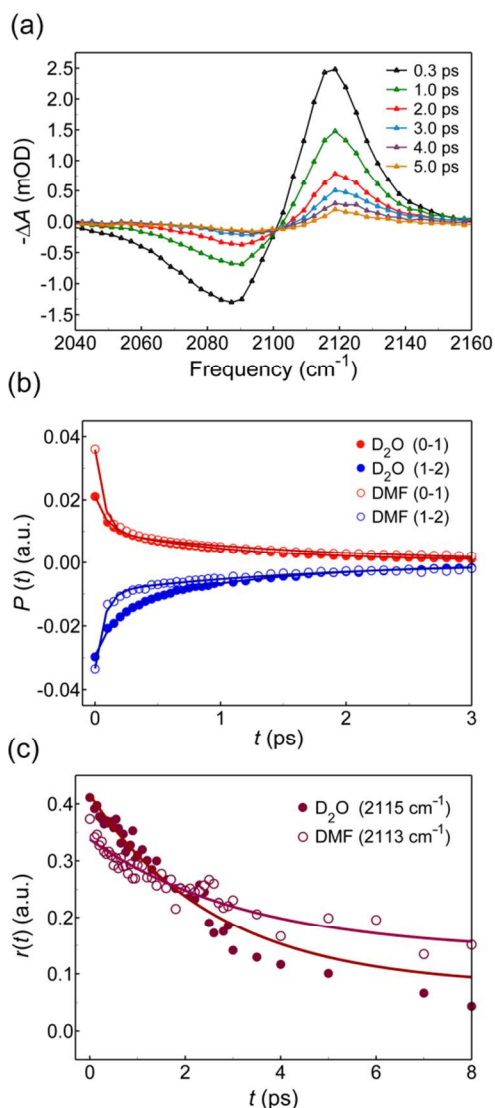


**Fig. 6** Polarization-controlled IR pump-probe data of **3**. (a) Isotropic IR pump-probe spectra of **3** in D<sub>2</sub>O at the delay time  $t$ . (b) Vibrational population decays of **3** in D<sub>2</sub>O and DMF. The integrated peak areas of the positive (0–1) and negative (1–2) peaks of the isotropic IR pump-probe spectra were fitted to a biexponential decay function for both D<sub>2</sub>O and DMF solutions. (c) Anisotropy decays of **3** in D<sub>2</sub>O and DMF. The anisotropy signals at the probe frequency were fitted to a single-exponential decay function for both D<sub>2</sub>O and DMF solutions. For the fitting parameters, see Table 1.

D<sub>2</sub>O compared to DMF. Perhaps, the lack of fast inertial orientational relaxation in D<sub>2</sub>O might be due to the strong H-bonding interaction of IR probe with surrounding water molecules in H-bonding network.

In H-bonding environments, the orientational diffusion has often been found to occur biexponentially, where the short time component originates from restricted orientational motion without breaking and reforming the H bonds with the vibrationally excited probe molecule. The biexponential decay of the anisotropy can be analysed by a wobbling-in-a-cone

model.<sup>70,71</sup> The details about the model can be found in Section S2 of the ESI.† One of the most meaningful parameters describing the degree of restriction on the wobbling-in-a-cone motion is the so called generalized order parameter  $Q$ , which can be easily obtained from the amplitude of the slow or fast component of the biexponential anisotropy decay. The parameter  $Q$  is equal to one for unrestricted motion and zero for fully restricted motion. We determined the parameter  $Q$  to be equal to 0.53 with semi-cone angle of 36.5° for **1** in D<sub>2</sub>O (Table S3 of the ESI†), which indicates a partially restricted orientational motion of the NC group. On the other hand, the single-exponential anisotropy decay of **3** in D<sub>2</sub>O indicates clearly different solvation structure and H-bonding pattern around the azido probe, resulting in substantially less restricted orientational diffusion and dominant contribution from the long-time complete orientational randomization.

Before closing the discussion about pump-probe data, it should be noted that the NC probe is particularly sensitive to its H-bonding interaction and dynamics. As shown in isotropic and anisotropic IR PP data analyses of the NC probe, both vibrational lifetime and orientational relaxation time constant show no notable difference between D<sub>2</sub>O and DMF, which suggests that the contribution of homogeneous broadening to the entire IR absorption bandwidth may be more or less the same. Thus, an increase in the bandwidth of the NC probe spectrum in D<sub>2</sub>O could reflect inhomogeneity of solvation structures with varying H-bond numbers and strengths. The interconversion dynamics among these hidden (spectrally unresolvable) structural variations could be studied by examining spectral diffusion dynamics measured using 2DIR method. With this large transition dipole strength and high sensitivity to H-bonding structure, we anticipate that the NC probe will become one of the popular probes for studying site-specific hydration structure of biological samples using 2DIR method in the future.

## Summary

In present work, we have studied the vibrational properties of NC-, CN- and N<sub>3</sub>-derivatized alanines **1–3** using FTIR and ultrafast IR pump-probe methods. From the FTIR spectra of **1–3**, we found that these IR probes have notably different sensitivities to H-bonding interactions. In addition, the dipole strength of the NC stretch mode is almost 5–40 times larger than that of the CN stretch mode. Moreover, the center frequency of the NC stretch

mode is red-shifted by  $\sim 100\text{ cm}^{-1}$  compared to that of the CN stretch mode, resulting in a large offset from the broad and intense OD band in  $\text{D}_2\text{O}$  solution, which makes it particularly better probe for nonlinear IR studies.

The ultrafast IR pump-probe experiments provided us information about the vibrational and rotational dynamics of **1** and **3**. Analyzing the time evolution of the integrated peak areas of the positive and negative pump-probe peaks, we determined the vibrational lifetimes of the NC stretch mode to be  $5.5 \pm 0.2\text{ ps}$  in both  $\text{D}_2\text{O}$  and DMF, which is several times longer than those of the azido stretch mode. In addition, the fact that the vibrational lifetime of the NC stretch mode in  $\text{D}_2\text{O}$  and DMF is identical indicates that the vibrational relaxation processes are mainly determined by intramolecular vibrational relaxation. The orientational relaxation time constants of the NC stretch mode were found to be  $0.52 \pm 0.20\text{ ps}$  and  $10.33 \pm 2.24\text{ ps}$  in  $\text{D}_2\text{O}$  and  $7.28 \pm 0.94\text{ ps}$  in DMF. The biexponential anisotropy decay was analysed using the wobbling-in-a-cone model and the degree of restriction on the orientational diffusion was discussed.

In summary, it is believed that the isonitrile stretch mode has the potential to be an excellent IR probe for studying the structure and dynamics of proteins. Moreover, it can also be used to probe the local electrostatic potential and its linear and nonlinear gradients because of its high sensitivity to local environment.

## Acknowledgements

This work was supported by IBS-R023-D1. H.H. is grateful for the financial support from the National Research Foundation of Korea (NRF) funded by the Ministry of Science, ICT, and Future Planning (NRF20110020033) and the Ministry of Education (NRF2013R1A1A2010933). K.K. thanks for the support from NRF of Korea (NRF2013R1A1A1010130). The IR pump-probe measurements were performed by using the multidimensional spectroscopy facility in the Seoul center of Korea Basic Science Institute (KBSI).

## Notes and references

<sup>a</sup> Center for Molecular Spectroscopy and Dynamics, Institute for Basic Science (IBS), Seoul 136-701, Korea. E-mail: mcho@korea.ac.kr.

<sup>b</sup> Department of Chemistry, Korea University, Seoul 136-701, Korea. E-mail: hogyuhan@korea.ac.kr

<sup>c</sup> Department of Chemistry, Chung-Ang University, Seoul 156-756, Korea

<sup>†</sup>These two authors contributed equally to this work.

<sup>†</sup> Electronic Supplementary Information (ESI) available: [detailed synthetic procedures and characterization for compounds, wobbling-in-a-cone model and tables and figures exhibiting the results of IR spectroscopic studies]. See DOI: 10.1039/b000000x/

1. H. Kim and M. Cho, *Chem Rev*, 2013, **113**, 5817-5847.
2. M. M. Waagele, R. M. Culik and F. Gai, *J. Phys. Chem. Lett.*, 2011, **2**, 2598-2609.
3. B. A. Lindquist, K. E. Furse and S. A. Corcelli, *Phys. Chem. Chem. Phys.*, 2009, **11**, 8119-8132.
4. S. Ye, E. Zaitseva, G. Caltabiano, G. F. X. Schertler, T. P. Sakmar, X. Deupi and R. Vogel, *Nature*, 2010, **464**, 1386-1389.
5. H. Taskent-Sezgin, J. Chung, P. S. Banerjee, S. Nagarajan, R. B. Dyer, I. Carrico and D. P. Raleigh, *Angew. Chem. Int. Ed.*, 2010, **49**, 7473-7475.
6. J. N. Bandaria, S. Dutta, S. E. Hill, A. Kohen and C. M. Cheatum, *J. Am. Chem. Soc.*, 2007, **130**, 22-23.
7. A. T. Krummel and M. T. Zanni, *J. Phys. Chem. B*, 2008, **112**, 1336-1338.
8. A. Remorino, I. V. Korendovych, Y. Wu, W. F. DeGrado and R. M. Hochstrasser, *Science*, 2011, **332**, 1206-1209.
9. C. Kolano, J. Helbing, M. Kozinski, W. Sander and P. Hamm, *Nature*, 2006, **444**, 469-472.
10. D. B. Strasfeld, Y. L. Ling, S.-H. Shim and M. T. Zanni, *J. Am. Chem. Soc.*, 2008, **130**, 6698-6699.
11. K. C. Schultz, L. Supekova, Y. Ryu, J. Xie, R. Perera and P. G. Schultz, *J. Am. Chem. Soc.*, 2006, **128**, 13984-13985.
12. S. S. Andrews and S. G. Boxer, *J Phys Chem A*, 2000, **104**, 11853-11863.
13. S. S. Andrews and S. G. Boxer, *J Phys Chem A*, 2001, **106**, 469-477.
14. M. M. Waagele, M. J. Tucker and F. Gai, *Chem. Phys. Lett.*, 2009, **478**, 249-253.
15. J.-H. Choi, D. Raleigh and M. Cho, *J. Phys. Chem. Lett.*, 2011, **2**, 2158-2162.
16. K.-I. Oh, W. Kim, C. Joo, D.-G. Yoo, H. Han, G.-S. Hwang and M. Cho, *J. Phys. Chem. B*, 2010, **114**, 13021-13029.
17. M. W. Nydegger, S. Dutta and C. M. Cheatum, *J. Chem. Phys.*, 2010, **133**, 134506.
18. K.-I. Oh, J.-H. Choi, J.-H. Lee, J.-B. Han, H. Lee and M. Cho, *J. Chem. Phys.*, 2008, **128**, 154504.
19. L. J. Webb and S. G. Boxer, *Biochemistry*, 2008, **47**, 1588-1598.
20. A. J. Stafford, D. L. Ensign and L. J. Webb, *J. Phys. Chem. B*, 2010, **114**, 15331-15344.
21. I. M. Pazos, R. M. Roesch and F. Gai, *Chem. Phys. Lett.*, 2013, **563**, 93-96.
22. H. Taskent-Sezgin, J. Chung, V. Patsalo, S. J. Miyake-Stoner, A. M. Miller, S. H. Brewer, R. A. Mehl, D. F. Green, D. P. Raleigh and I. Carrico, *Biochemistry*, 2009, **48**, 9040-9046.
23. H. Taskent-Sezgin, P. Marek, R. Thomas, D. Goldberg, J. Chung, I. Carrico and D. P. Raleigh, *Biochemistry*, 2010, **49**, 6290-6295.
24. Z. Getahun, C.-Y. Huang, T. Wang, B. De León, W. F. DeGrado and F. Gai, *J. Am. Chem. Soc.*, 2002, **125**, 405-411.
25. K. I. Oh, J. H. Lee, C. Joo, H. Han and M. Cho, *J. Phys. Chem. B*, 2008, **112**, 10352-10357.
26. X. S. Gai, B. A. Coutifaris, S. H. Brewer and E. E. Fenlon, *Phys. Chem. Chem. Phys.*, 2011, **13**, 5926-5930.
27. L. Edelstein, M. A. Stetz, H. A. McMahon and C. H. Londergan, *J. Phys. Chem. B*, 2010, **114**, 4931-4936.
28. A. T. Fafarman, L. J. Webb, J. I. Chuang and S. G. Boxer, *J. Am. Chem. Soc.*, 2006, **128**, 13356-13357.
29. D. M. Walker, E. C. Hayes and L. J. Webb, *Phys. Chem. Chem. Phys.*, 2013, **15**, 12241-12252.
30. D. M. Walker, R. Wang and L. J. Webb, *Phys. Chem. Chem. Phys.*, 2014, **16**, 20047-20060.
31. H. A. McMahon, K. N. Alfieri, K. A. A. Clark and C. H. Londergan, *J. Phys. Chem. Lett.*, 2010, **1**, 850-855.
32. K.-H. Park, J. Jeon, Y. Park, S. Lee, H.-J. Kwon, C. Joo, S. Park, H. Han and M. Cho, *J. Phys. Chem. Lett.*, 2013, **4**, 2105-2110.
33. J. H. Choi, K. I. Oh and M. H. Cho, *J. Chem. Phys.*, 2008, **129**, 174512.
34. K. K. Lee, K. H. Park, C. Joo, H. J. Kwon, J. Jeon, H. I. Jung, S. Park, H. Han and M. Cho, *J. Phys. Chem. B*, 2012, **116**, 5097-5110.

35. S. Dutta, Y.-L. Li, W. Rock, J. C. D. Houtman, A. Kohen and C. M. Cheatum, *J. Phys. Chem. B*, 2011, **116**, 542-548.
36. S. Dutta, W. Rock, R. J. Cook, A. Kohen and C. M. Cheatum, *J. Chem. Phys.*, 2011, **135**, 055106.
37. M. C. Thielges, J. Y. Axup, D. Wong, H. S. Lee, J. K. Chung, P. G. Schultz and M. D. Fayer, *J. Phys. Chem. B*, 2011, **115**, 11294-11304.
38. M. J. Tucker, X. S. Gai, E. E. Fenlon, S. H. Brewer and R. M. Hochstrasser, *Phys. Chem. Chem. Phys.*, 2011, **13**, 2237-2241.
39. K. L. Kiick, E. Saxon, D. A. Tirrell and C. R. Bertozzi, *Proc. Natl. Acad. Sci. U.S.A.*, 2002, **99**, 19-24.
40. H. M. Mueller-Werkmeister, K. Eberl, M. Essig and J. Bredenbeck, *Biophys. J.* 2013, **104**, 29a.
41. R. Bloem, K. Koziol, S. A. Waldauer, B. Buchli, R. Walser, B. Samatanga, I. Jelesarov and P. Hamm, *J. Phys. Chem. B*, 2012, **116**, 13705-13712.
42. J. Helbing, *Chem. Phys.*, 2012, **396**, 17-22.
43. M. Lim, P. Hamm and R. M. Hochstrasser, *Proc. Natl. Acad. Sci. U.S.A.*, 1998, **95**, 15315-15320.
44. J. N. Bandaria, S. Dutta, M. W. Nydegger, W. Rock, A. Kohen and C. M. Cheatum, *Proc. Natl. Acad. Sci. U.S.A.*, 2010, **107**, 17974-17979.
45. R. Adhikary, J. Zimmermann, P. E. Dawson and F. E. Romesberg, *ChemPhysChem*, 2014, **15**, 849-853.
46. K. K. Lee, K. H. Park, C. Joo, H. J. Kwon, H. Han, J. H. Ha, S. Park and M. Cho, *Chem. Phys.*, 2012, **396**, 23-29.
47. E. Lieber, C. N. R. Rao, A. E. Thomas, E. Oftedahl, R. Minnis and C. V. N. Nambury, *Spectrochim. Acta*, 1963, **19**, 1135-1144.
48. L. Dyal and J. Kemp, *Aust. J. Chem.*, 1967, **20**, 1395-1402.
49. J. S. Lipkin, R. Song, E. E. Fenlon and S. H. Brewer, *J. Phys. Chem. Lett.*, 2011, **2**, 1672-1676.
50. A. Tokmakoff, B. Sauter and M. D. Fayer, *J. Chem. Phys.*, 1994, **100**, 9035-9043.
51. S. K. K. Kumar, A. Tamimi and M. D. Fayer, *J. Am. Chem. Soc.*, 2013, **135**, 5118-5126.
52. O. Kel, A. Tamimi, M. C. Thielges and M. D. Fayer, *J. Am. Chem. Soc.*, 2013, **135**, 11063-11074.
53. O. Kel, A. Tamimi and M. D. Fayer, *Proc. Natl. Acad. Sci. U.S.A.*, 2014, **111**, 918-923.
54. I. Peran, T. Oudenhoven, A. M. Woys, M. D. Watson, T. O. Zhang, I. Carrico, M. T. Zanni and D. P. Raleigh, *J. Phys. Chem. B*, 2014, **118**, 7946-7953.
55. A. M. Woys, S. S. Mukherjee, D. R. Skoff, S. D. Moran and M. T. Zanni, *J. Phys. Chem. B*, 2013, **117**, 5009-5018.
56. D. E. Moilanen, I. R. Piletic and M. D. Fayer, *J. Phys. Chem. C*, 2007, **111**, 8884-8891.
57. N. M. Levinson, S. D. Fried and S. G. Boxer, *J. Phys. Chem. B*, 2012, **116**, 10470-10476.
58. M. J. Kamlet, J. L. M. Abboud, M. H. Abraham and R. W. Taft, *J. Org. Chem.*, 1983, **48**, 2877-2887.
59. Y. S. Kim and R. M. Hochstrasser, *Proc. Natl. Acad. Sci. U.S.A.*, 2005, **102**, 11185-11190.
60. M. Heger, T. Scharge and M. A. Suhm, *Phys. Chem. Chem. Phys.*, 2013, **15**, 16065-16073.
61. A. S. Hansen, L. Du and H. G. Kjaergaard, *Phys. Chem. Chem. Phys.*, 2014, **16**, 22882-22891.
62. S. Bagchi, S. D. Fried and S. G. Boxer, *J. Am. Chem. Soc.*, 2012, **134**, 10373-10376.
63. A. B. McCoy, *J. Phys. Chem. B*, 2014, **118**, 8286-8294.
64. L. Chieffo, J. Shattuck, J. J. Amsden, S. Erramilli and L. D. Ziegler, *Chem. Phys.*, 2007, **341**, 71-80.
65. I. T. Suydam and S. G. Boxer, *Biochemistry*, 2003, **42**, 12050-12055.
66. H. Son, K. H. Park, K. W. Kwak, S. Park and M. Cho, *Chem. Phys.*, 2013, **422**, 37-46.
67. S. Bagchi, S. G. Boxer and M. D. Fayer, *J. Phys. Chem. B*, 2012, **116**, 4034-4042.
68. D. C. Urbanek, D. Y. Vorobyev, A. L. Serrano, F. Gai and R. M. Hochstrasser, *J. Phys. Chem. Lett.*, 2010, **1**, 3311-3315.
69. C. Fang, J. D. Bauman, K. Das, A. Remorino, E. Arnold and R. M. Hochstrasser, *Proc. Natl. Acad. Sci. U.S.A.*, 2008, **105**, 1472-1477.
70. S. Park, D. E. Moilanen and M. D. Fayer, *J. Phys. Chem. B*, 2008, **112**, 5279-5290.
71. G. Lipari and A. Szabo, *Biophys. J.* 1980, **30**, 489-506.
72. X. H. Qu, E. A. Lee, G. S. Yu, T. B. Freedman and L. A. Nafie, *Appl. Spectrosc.*, 1996, **5**, 649-557.